GAN-GENERATED ELEVATION MODELS IN COMPUTATIONAL FLUID DYNAMICS: A FEASIBILITY STUDY FOR COMPLEX URBAN TERRAIN

Maximilian Langheinrich[1], Ksenia Bittner[1], Peter Reinartz[1]

[1] Remote Sensing Technology Institute, German Aerospace Center (DLR), Wessling, Germany - (maximilian.langheinrich, ksenia.bittner, peter.reinartz)@dlr.de

ABSTRACT

Recently developed methods to simulate *very high-resolution (VHR)* wind fields over complex urban terrain rely on high-quality three-dimensional vector representations of building information. Unfortunately data of that kind is sparsely available on a worldwide scale. In this work, we investigate the applicability of *computational fluid dynamics (CFD)* on 2.5D *digital surface models (DSMs)* automatically generated by *generative adversarial network (GAN)* from globally available satellite data which includes photogrammetric DSMs and *pan-chromatic (PAN)* images. The obtained results demonstrate that the GAN-based DSMs are reasonable alternatives to rarely available *level of detail 2 (LoD2)* vector data, promoting large coverage, continuous wind field derivation over complex terrain.

Index Terms— computational fluid dynamic, Reynolds-averaged Navier-Stokes, detached-eddy simulation, OpenFOAM, complex urban terrain, digital surface model, generative adversarial network

1. INTRODUCTION

With intensive development of deep learning techniques, nowadays it is not only possible to categorize each pixel in an image with a high degree of accuracy but also to reconstruct the continuous values in the form of meaningful geometries. Specifically, the recently developed *conditional generative adversarial network (cGAN)* model [1] is able to generate DSMs with improved building shapes in comparison to the initial low-quality photogrammetric DSMs computed from stereo satellite imagery. The availability of good-quality DSMs is an essential part for many geoscientific applications. In the field of remote sensing they can be used *e.g.*, to correct for height and topography dependent radiative transfer effects [2], to reduce distortion effects in satellite images by means of orthorectification or to derive second level products like 3D city models.

Regarding 3D city models generation, it was recently shown [3][4] that fused, VHR DSMs (generated from *digital terrain models (DTMs)* and LoD2 building models) can be utilized as input to fluid dynamics computations in order to simulate three-dimensional wind fields in complex urban environments. In order to guarantee a continuously stable solution of the Navier-Stokes equations of the turbulent flow of air, the underlying input geometry has to be of high-quality in terms of certain mesh quality metrics.

The experiments presented in this paper assess the eligibility of DSMs, automatically generated by the cGAN model, for CFD calculations in comparison to high-quality, handcrafted input geometries.

2. METHODOLOGY

2.1. cGAN

It has been already investigated [1, 5] that GANs [6], initially developed for different domain adaptation problems, are also applicable for remote sensing tasks, such as the optimization of low-quality photogrammetric DSMs with reduced effort comparing to traditional filtering [7] or interpolation [8] techniques. Moreover, Bittner *et al.* [1] demonstrated that the integration of height information from the initial photogrammetric DSM with intensity information from the PAN image at the earlier stage of the neural network architecture allows to reconstruct more complete building structures with even sharper roof ridge lines. Resulting height images contain a better representation of building shapes with clearly defined roof structures. On the other hand, the vegetation is eliminated in the resulting DSM as the ground truth elevation model is generated from *city geography markup language (CityGML)* data which contains building representations of LoD2 in our case. The DSM generated by Bittner *et al.* [1] methodology is the input to CFD.

2.2. Turbulence models

Two different turbulence models are used in consecutive order during the CFD calculation. To get the first estimate of the mean wind field over the test geometry, a *Reynolds-averaged Navier-Stokes (RANS)* [9] simulation is applied to iteratively solve for an incompressible, steady-state solution of the turbulent flow of air. To enable the analysis of transient, small scale turbulence in complex urban terrain, in the second step,

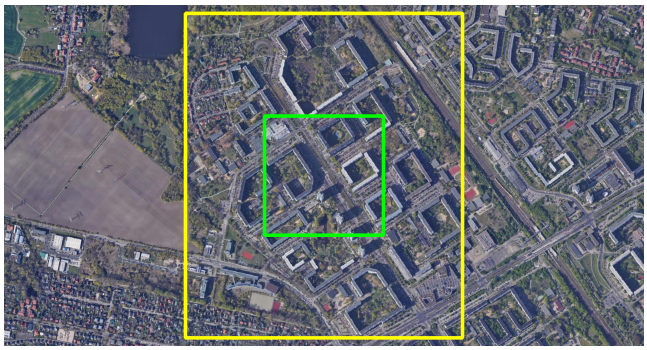

Fig. 1: Boundaries for AOI (green) and atmospheric boundary field (yellow) depicted in GoogleMaps engine.

a *Detached-eddy simulation (DES)* is calculated. The DES represents a combination of the common approaches of *Large eddy simulation (LES)* and RANS and is realized in form of the *Spalart-Allmaras DDES* model [10]. For an in-depth clarification of the underlying theory please refer to the respective references.

3. DATA

The *area of interest (AOI)* observed in the experiments covers 500×500 m^2 in a strongly urbanized area located in the northeast of Berlin, Germany. The horizontal size of all prepared datasets is extended by 332 m in x- and 431 m in y-dimension, to enable the calculation of CFD for the area outside of the AOI in order to ensure correctly developed atmospheric boundary conditions. Figure 1 shows the bounding rectangles for the AOI and the extended region.

This particular region was chosen as it features a composition of high-rise, partly open building complexes as well as large street canyons. Both types of structures promote the formation of small scale amplification effects by acting as natural wind tunnels and therefore cause local changes in the wind field that can not be observed in wind speed maps of lower resolution or regions with open topographies. Further the more complex geometries enable a better assessment of the meshing quality concerning the two compared approaches.

The data is used in the CFD process in form of 3D meshes generated with Delaunay triangulation. For each test case the particular mesh was constructed from a point cloud. For one dataset the output DSM of the cGAN approach discussed in Section 2.1 was used. The other mesh was generated from a fused DTM + LoD2 point cloud sourced from publicly available surveying data. Both source datasets feature a spatial resolution of 0.5 m in *ground sampling distance (GSD)*.

4. EXPERIMENTS

To conduct the calculation of three-dimensional wind fields over the AOI, the OpenFOAM [11] framework was used. The processing pipeline consists of two major steps:

- *Meshing of finite-element volume*: The 3D atmospheric volume around and above the AOI geometry was generated and divided into volumetric cells for which the second processing step was conducted. The quality of the atmospheric boundary mesh is essential for the calculation of the Navier-Stokes equations of turbulent flow.
- *Calculation of three-dimensional wind field*: The coupled solution for the model is calculated on basis of a finite-element approach. In the experiments, two different turbulence models described in Section 2.2 are applied consecutively, with the converged solution of the RANS calculation posing as an initial state for the DES processing.

The boundary conditions for the extended area inlet surface (left edge of the yellow rectangle in Figure 1) are $p = 1013.25$ hPa, $U = 35\,\mathrm{m\,s^{-1}}$ at reference height $zref = 10$ m above ground, $\nu_t = 0.0$, $\tilde{\nu} = 0.01$. The values for k and ϵ are calculated automatically as a function of the inlet boundary vertical wind profile.

Calculations were conducted in parallel on 20 processors resulting in a mean meshing time of 46 min and mean calculation times of 3.5 h and 132 h for the RANS and DES models accordingly. For the former, the simulation converged to the results over 400 iteration steps, for the latter, a solution was calculated for every 0.01 s over a period of 60 s, while saving the state every second.

5. RESULTS

5.1. Mesh quality

The general mesh quality is evaluated by means of three quality metrics:

- *Total number of cells* included in the atmospheric boundary volume.
- *Non-orthogonality*: Angle between the line connecting two cell centers and the normal of their common face. 0.0° represents the best value with a maximum validity threshold of 65.0°.
- *Skewness*: Distance between the intersection of the line connecting two cell centers with their common face and the center of that face. Cell pairs with smaller skewness values bear a higher quality with 4.0 m being the maximum tolerable threshold.

Results for all cell pairs in the atmospheric volume are needed and are obtained using the *checkMesh* utility provided by the OpenFOAM framework. Table 1 shows total cell numbers, average non-orthogonality and maximum skewness for the different approaches.

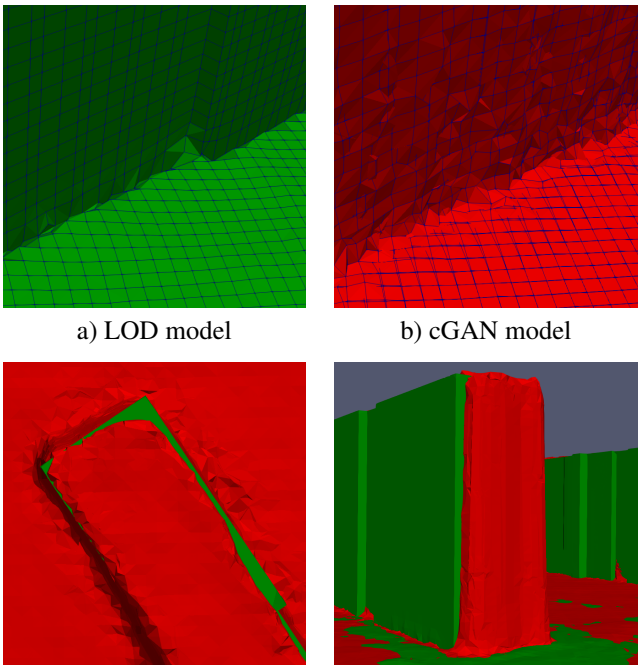

a) LOD model b) cGAN model

c) Building outlines d) Building edge slope

Fig. 2: Inherent mesh differences.

	LOD Model	GAN Model
Overall cell #	30324762	32517019
Avg. Non-orthogonality	2.43	3.13
Max. Skewness	9.20 (12)	9.61 (54)

Table 1: Quality metrics for the atmospheric boundary meshes. The two values in brackets show the count of cells exceeding the skewness threshold of 4.0 m.

While the two meshes are of comparable overall quality (the percentage of skewed faces of LOD: 3.9e-5 % and GAN: 16×10^{-5} % being neglectable) and therefore in both cases generally suitable for a successful CFD calculation, there are inherent differences between the two models that can be detected by visual inspection.

These differences are caused by the different composition of the underlying input data. While the mesh generated from the fused DSM + LoD2 model exhibits true 3D data (able to feature multiple height values for the same coordinate), the GAN mesh originates from a rasterized, 2.5D image with a single height value for every pixel. This on the one hand results in sloped building walls for the GAN case, as mesh points on the bottom and the top of a building wall can not coincide at the same vertical geo-coordinate. This can be seen in Figure 2d. Further the overall composition of building boundaries in the GAN mesh is more coarse compared to the clean surfaces of the vector based LoD2 model (Figure 2c). This again is caused by the stepwise realized building edges in the underlying raster dataset. The roughness also induces the difference in the overall cell count as shown in Table 1 as more cells are needed to approximate rough wall surfaces (Figure 2 a and b).

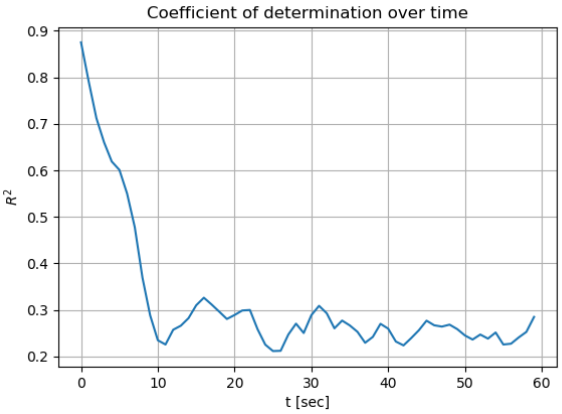

Fig. 3: Correlation of transient wind fields over time.

5.2. Wind field simulation

The analysis of the steady-state and transient wind fields resulting from the CFD calculations is conducted on an atmospheric layer 10 m above ground covering the 500×500 m^2 horizontal extent of the AOI and therefore for 250000 datapoints.

Figure 3 shows the development of the R^2 values between the DES GAN model and the reference LoD2 based model, with $t = 0$ representing the converged steady-state of the RANS simulation. While the initial states of both approaches strongly correlate with each other, the alignment of the calculated wind speeds rapidly decreases within the first 10 s of the transient solution with a further decreasing trend reaching the last simulated time step.

This behaviour is a consequence of the geometrical inconsistencies described in Section 5.1. For the initial state, large deviations between the calculated wind speeds primarily occur near building walls and narrow passages in flow direction. The effect can be seen in Figure 5 and 4 (left image). As the solution of the three-dimensional Navier-Stokes equations represents a coupled system, these initial local errors propagate over the temporal evolution of the simulation, raising the overall mean absolute error from 3.32 m s^{-1} to 8.19 m s^{-1} and distributing local turbulence difference over the whole extents of the AOI (Figure 4 / right image).

6. CONCLUSION

The on hand comparison of meshes generated from point clouds based on high-resolution elevation models derived by a *generative adversarial network (GAN)* and vector based *level of detail 2 (LoD2)* building models and their evaluation

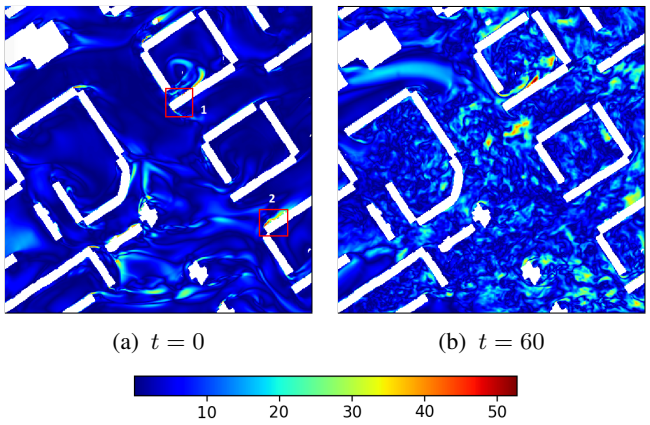

(a) $t = 0$ (b) $t = 60$

Fig. 4: Absolute error per pixel for time $t = 0$ s and $t = 60$ s.

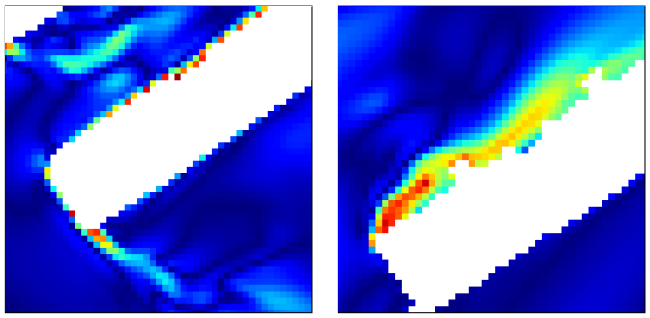

(a) Example 1 (b) Example 2

Fig. 5: Examples of absolute error representation at wall and corner regions of two building geometries ("1" and "2"), highlighted by red squares in Figure 4. Scale in m s^{-1}.

in terms of usability in wind speed simulations show that: a) Both approaches are geared for the generation of atmospheric boundary volumes as used in *computational fluid dynamics (CFD)* processing, featuring comparable mesh quality; b) The inherent coarseness of the GAN model geometries promote the formation of local errors, especially near buildings and narrow passages, that lead to a growing inaccuracy over time. The latter insight only applies to the solutions of the transient *Detached-eddy simulation (DES)* turbulence model. Regarding the converged results of the steady-state *Reynolds-averaged Navier-Stokes (RANS)* turbulence model, the wind fields correlate in large parts. This renders the GAN derived models an attractive and feasible alternative to the time consuming process of manual high-quality mesh generation. The largest advantage of the former is the global availability of input data (in form of multi-spectral / *pan-chromatic (PAN)* satellite images and *digital surface models (DSMs)*) in comparison to the scarcely provided, high-quality LoD2 data. This enables the large scale generation of continuous, high resolution wind fields that can be used in applications related to *i.e.*, renewable energy, natural hazards and atmospheric particle dispersion. At this point both methodologies, the GAN DSM generation and the CFD pipeline, can be developed further to increase accuracy *i.e.*, by respectively refining and smoothing the building shape and/or modelling the atmospheric boundary conditions in more detail. This will be subject to future investigations.

References

[1] K. Bittner, P. Reinartz, and M. Korner, "Late or earlier information fusion from depth and spectral data? large-scale digital surface model refinement by hybrid-cgan," in *Proceedings of the IEEE Conference on Computer Vision and Pattern Recognition Workshops*, 2019.

[2] R. Richter, "Correction of satellite imagery over mountainous terrain," *Applied optics*, vol. 37, no. 18, pp. 4004–4015, 1998.

[3] M. Langheinrich, P. Fischer, and T. Krauß, "Modeling wind flow over complex urban terrain," in *2017 Joint Urban Remote Sensing Event (JURSE)*, IEEE, 2017, pp. 1–4.

[4] M. Langheinrich and K. Seifert, "An advanced workflow for simulating high resolution wind fields over complex urban terrain including single tree objects," in *IGARSS 2019-2019 IEEE International Geoscience and Remote Sensing Symposium*, IEEE, 2019, pp. 7657–7660.

[5] K. Bittner, P. d'Angelo, M. Körner, and P. Reinartz, "Dsm-to-lod2: Spaceborne stereo digital surface model refinement," *Remote Sensing*, vol. 10, no. 12, p. 1926, 2018.

[6] I. Goodfellow, J. Pouget-Abadie, M. Mirza, B. Xu, D. Warde-Farley, S. Ozair, A. Courville, and Y. Bengio, "Generative adversarial nets," in *Advances in Neural Information Processing Systems (NIPS)*, 2014, pp. 2672–2680.

[7] A. M. Felicísimo, "Parametric statistical method for error detection in digital elevation models," *ISPRS Journal of Photogrammetry and Remote Sensing*, vol. 49, no. 4, pp. 29–33, 1994.

[8] E. Anderson, J. Thompson, and R. Austin, "Lidar density and linear interpolator effects on elevation estimates," *International Journal of Remote Sensing*, vol. 26, no. 18, pp. 3889–3900, 2005.

[9] B. E. Launder and D. B. Spalding, "The numerical computation of turbulent flows," in *Numerical prediction of flow, heat transfer, turbulence and combustion*, Elsevier, 1983, pp. 96–116.

[10] P. R. Spalart, S. Deck, M. L. Shur, K. D. Squires, M. K. Strelets, and A. Travin, "A new version of detached-eddy simulation, resistant to ambiguous grid densities," *Theoretical and computational fluid dynamics*, vol. 20, no. 3, p. 181, 2006.

[11] H. Jasak, A. Jemcov, Z. Tukovic, *et al.*, "Openfoam: A c++ library for complex physics simulations," in *International workshop on coupled methods in numerical dynamics*, IUC Dubrovnik Croatia, vol. 1000, 2007, pp. 1–20.